EGAN 2011 Workshop -- Padova 26–30/06/2011

Lifetime measurement of the 6.792 MeV state in ^{15}O with the AGATA Demonstrator

R. Depalo[1], C. Michelagnoli[2,3], R. Menegazzo[2], C. A. Ur[2], D. Bazzacco[2], D.Bemmerer[4], C. Broggini[2], A. Caciolli[2,5], M. Erhard[4], E. Farnea[2], F. Filmer[6], Zs. Fülöp[7], A. Gottardo[1], R. S. Kempley[8], M. Marta[4], R. McAdoo[1], D. Mengoni[2,3], T. Mijatović[9], G. Pollarolo[10], F. Recchia[2], C. Rossi Alvarez[2], E. Sahin[1], T. Szücs[9], J.J. Valiente-Dobon[1], N. Keeley[10]
the AGATA collaboration

[1] INFN, Sezione di Legnaro, Legnaro (Padova), Italy. [2] INFN, Sezione di Padova, Padova, Italy.
[3] Dipartimento di Fisica dell'Universit` di Padova, Padova, Italy.
[4] Helmholtz-Zentrum Dresden-Rossendorf, Dresden, Germany.
[5] CGT, San Giovanni Valdarno and University of Siena. [6] University of Liverpool, Liverpool, UK.
[7] ATOMKI, Debrecen, Hungary. [8] Department of Physics of the University of Surrey, Guildford, UK.
[9] Ruder Boˇ kovi´ Institute, Zagreb, Croatia. [10] INFN and Universit` di Torino, Torino, Italy.
[10]Department of Nuclear Reactions, The Andrzej Sołtan Institute for Nuclear Studies, Warsaw, Poland

The solar composition problem

Recent determination of solar abundances, based on new 3D solar atmosphere models, imply a 30% decrease in Z/X: from **0.0229** (Grevesse & Sauval, 1998) to **0.0165** (Asplund, Grevesse & Sauval, 2005)

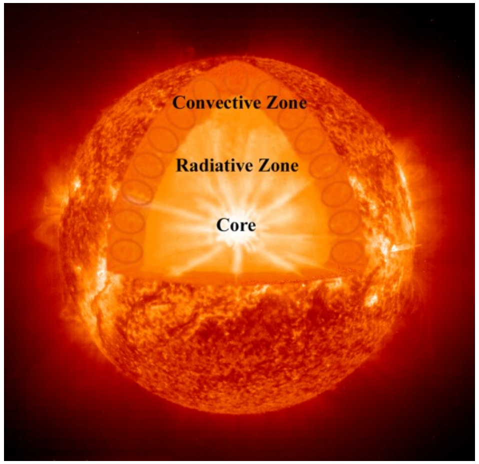

- Sound speed and density profile in disagreement with helioseismological measurements
- Central temperature lowered by 1.2% ➡ 21% decrease in ^{8}B ν flux
- Smaller temperature gradient ➡ $R_{CZ}/R_{☼}$ from 0.713 to 0.728
- Age of globular clusters increased by 5 - 10%
- 40% decrease in CNO ν flux (E < 2MeV)

The solar composition problem

CNO neutrinos provide an independent evaluation of C and N abundances in the solar core...BUT...CNO reactions cross sections should be accurately known!

The $^{14}N(p,\gamma)^{15}O$ reaction is the slowest one, thus determining the overall rate

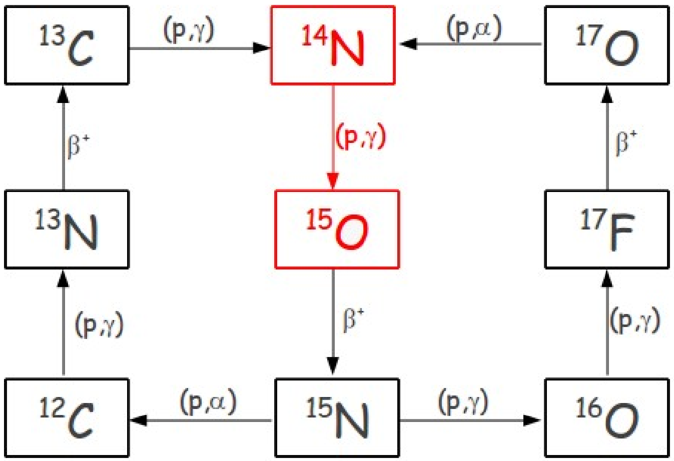

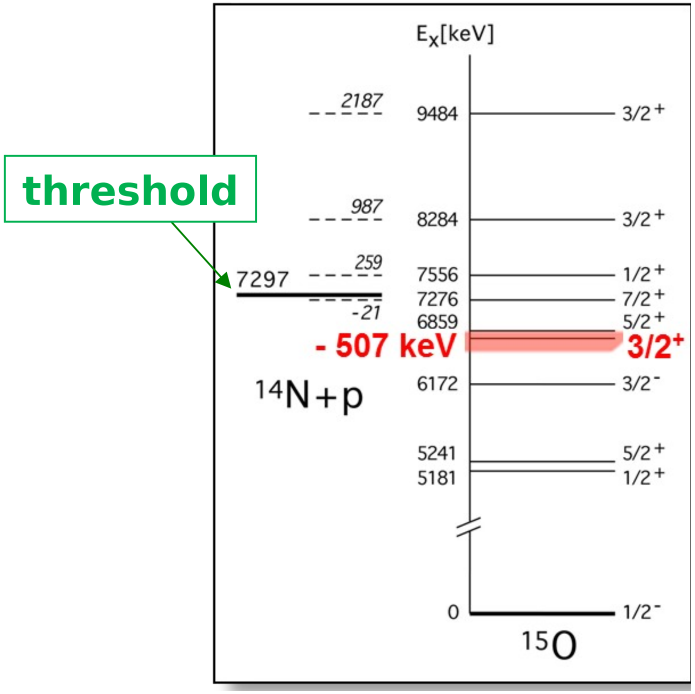

When extrapolating the cross section to the Gamow peak energy window (~30 keV), sub-threshold resonances corresponding to bound states in ^{15}O have to be taken into account

The $^{14}N(p,\gamma)^{15}O$ cross section is determinated largely by the transition to the 6.79 MeV ($3/2^+$) state in ^{15}O (now measured down to 70 keV)

Lifetime of the 6.79 MeV state

Group	Method	$\tau_\gamma^{6.792}$ [fs]
Oxford 1968 W.Gill et al., Nucl. Phys. A 121. 209	DSAM d(^{14}N, ^{15}0)n	< 28
TUNL 2001 P.F. Bertone et al., Phys. Rev. Lett. 87, 152501	DSAM ^{14}N(p,γ)^{15}O	1.6±0.7 (44%)
RIKEN 2004 K. Yamada et al., Phys. Lett. B 579, 265	CE ^{208}Pb(^{15}O, ^{15}O*)	0.69±0.43 (62%)
LUNA 2004 A. Formicola et al., Phys. Lett. B 591, 61	Cross section + R-matrix fit	1.1±0.5 (45%)
TUNL 2005 R. Runkle et al., Phys. Rev. Let. 94, 082503	Cross section + R-matrix fit	0.3±0.1 (33%)
Bochum 2008 D. Schürmann et al., Phys. Rev. C 77, 055803	DSAM ^{14}N(p,γ)^{15}O	< 0.77
LUNA 2008 M. Marta et al., Phys. Rev. C 78, 022802(R)	Cross section + R-matrix fit	0.75±0.20 (27%)

The uncertainity on the resonance width is still too high!

Lifetime of the 6.79 MeV state

Group	Method	$\tau_\gamma^{6.792}$ [fs]
Oxford 1968 W.Gill et al., Nucl. Phys. A 121. 209	DSAM $d(^{14}N, ^{15}O)n$	< 28
TUNL 2001 P.F. Bertone et al., Phys. Rev. Lett. 87, 152501	DSAM $^{14}N(p,\gamma)^{15}O$	1.6±0.7 (44%)
RIKEN 2004 K. Yamada et al., Phys. Lett. B 579, 265	CE $^{208}Pb(^{15}O, ^{15}O^*)$	0.69±0.43 (62%)
LUNA 2004 A. Formicola et al., Phys. Lett. B 591, 61	Cross section + R-matrix fit	1.1±0.5 (45%)
TUNL 2005 R. Runkle et al., Phys. Rev. Let. 94, 082503	Cross section + R-matrix fit	0.3±0.1 (33%)
Bochum 2008 D. Schürmann et al., Phys. Rev. C 77, 055803	DSAM $^{14}N(p,\gamma)^{15}O$	< 0.77
LUNA 2008 M. Marta et al., Phys. Rev. C 78, 022802(R)	Cross section + R-matrix fit	0.75±0.20 (27%)

The uncertainity on the resonance width is still too high!

Measurement of the lifetime of the 6.79 MeV state in ^{15}O with the DSAM using the AGATA Demonstrator

Reaction $^2H(^{14}N,n)^{15}O$ (Q = 5.072 MeV) in inverse kinematics

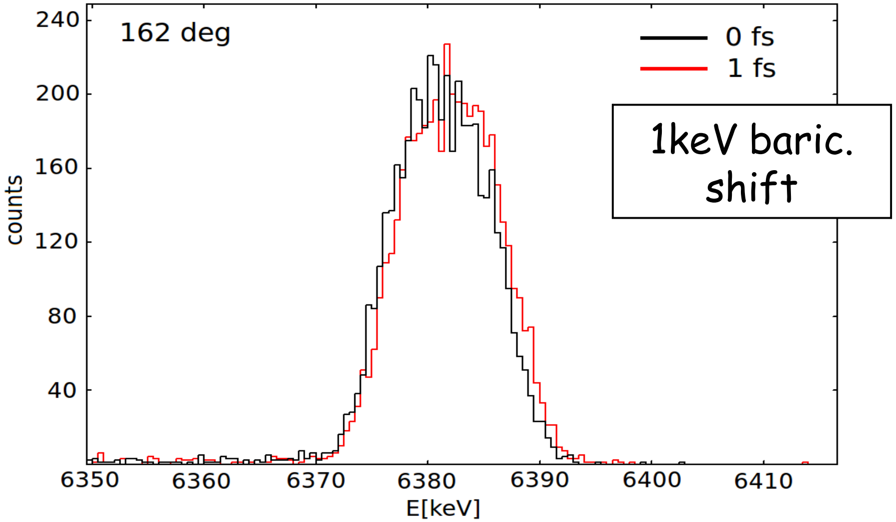

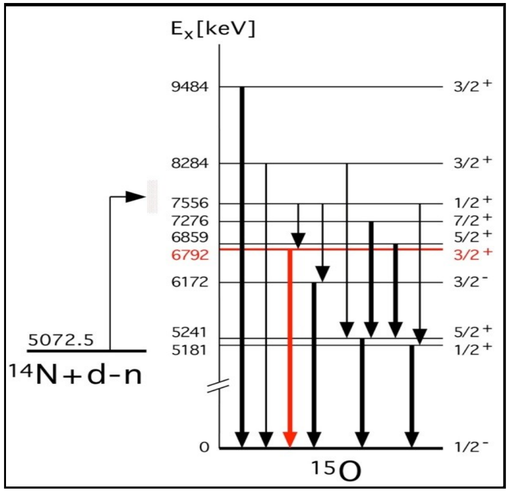

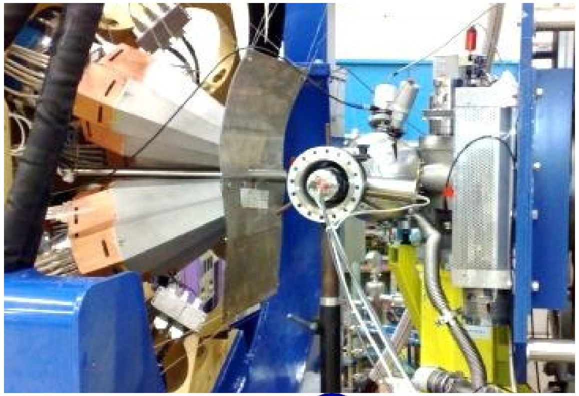

- **Reaction $^{2}H(^{14}N,n)^{15}O$ @ 32 MeV**
  Tandem XTU terminal voltage 8.95 MV
  $I(^{14}N^{3+})$ ~ 4 - 5 pnA

- **^{2}H implanted in a thin surface layer of a 4mg/cm^{2} Au target**

- **AGATA Demonstrator (4ATC's) at backward angles**

Crystal	θ [deg]
R	168.54
G	159.99
B	156.57

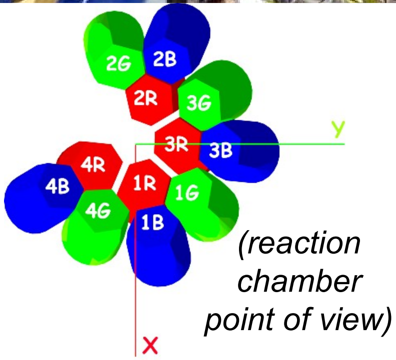

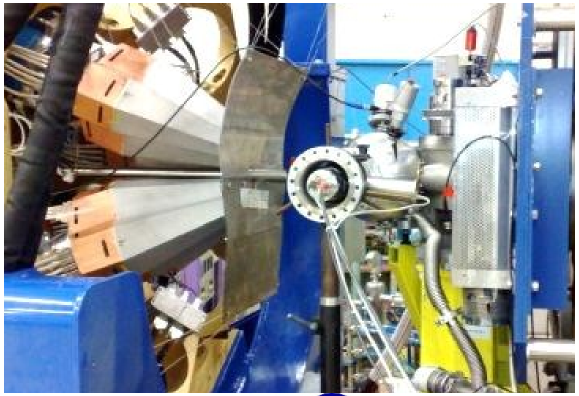

- **Reaction $^{2}H(^{14}N,n)^{15}O$ @ 32 MeV**
  Tandem XTU terminal voltage 8.95 MV
  $I(^{14}N^{3+})$ ~ 4 - 5 pnA

- **^{2}H implanted in a thin surface layer of a 4mg/cm^2 Au target**

- **AGATA Demonstrator (4ATC's) at backward angles**

Crystal	θ [deg]
R	168.54
G	159.99
B	156.57

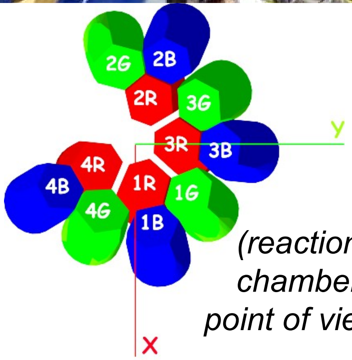

(reaction chamber point of view)

$\beta(^{15}O)$ ~ 6.5 % ; E_0 = 6791.4 keV

$$E(\vartheta) = E_0 \frac{\sqrt{1-\beta^2}}{1-\beta\cos\vartheta} = 6384 \text{ keV}$$

→ low gain of the electronics (20 MeV dynam. range)

- **AmBe(Fe) source during experiment to monitor gain stability**
  (~60 cm below the reaction chamber)

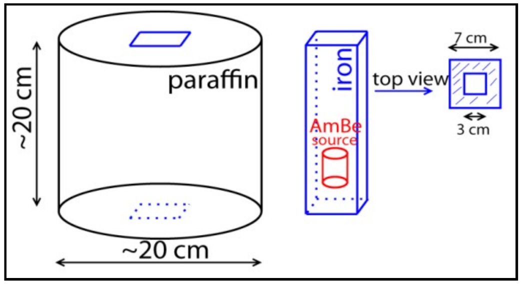

Data analysis: data processing

- Energy calibration of CC and segments with high energy gammas
  - Off-line refinement was needed to align the CC spectra
  - Non linearity of segments signals in the low gain range

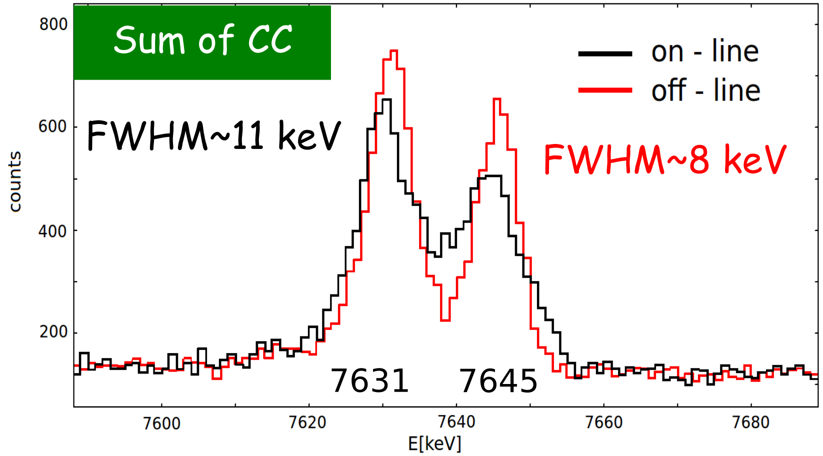

- Tracking performed forcing the sum of the energy releases of the tracked points to be equal to the corresponding energy seen in the CC

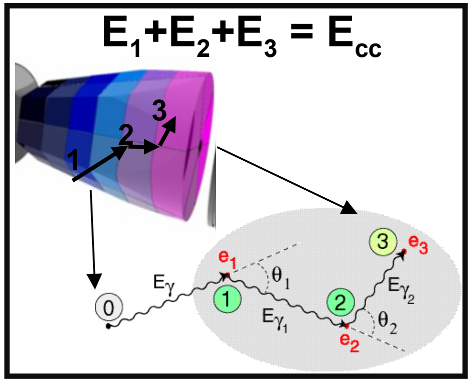

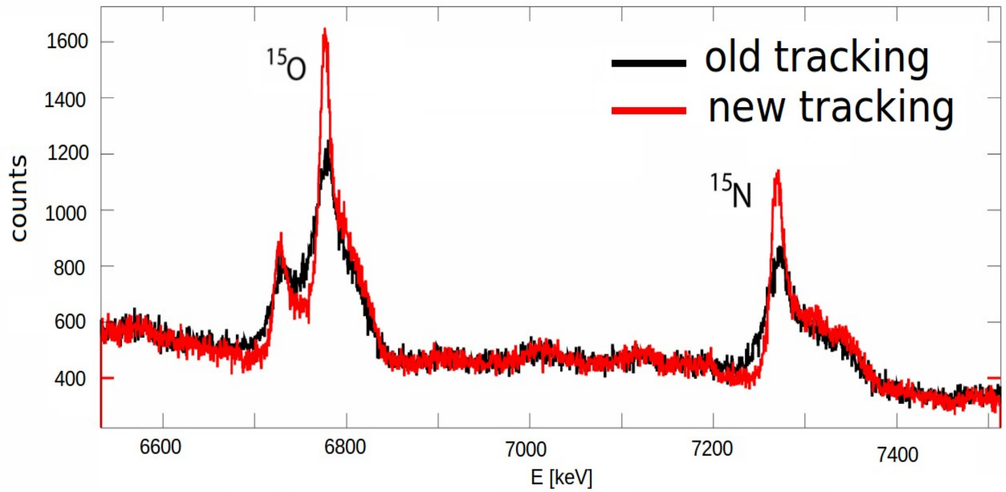

The angular range can be splitted into 2° slices according to the angle of the first interaction point (identified by the tracking algorithm)

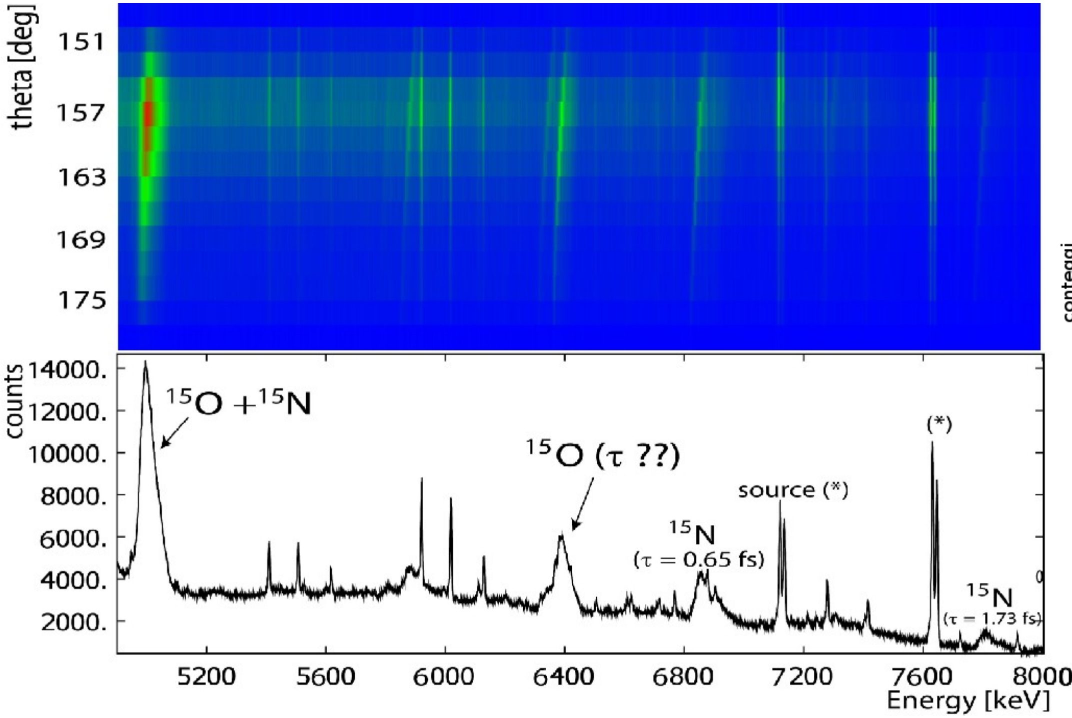

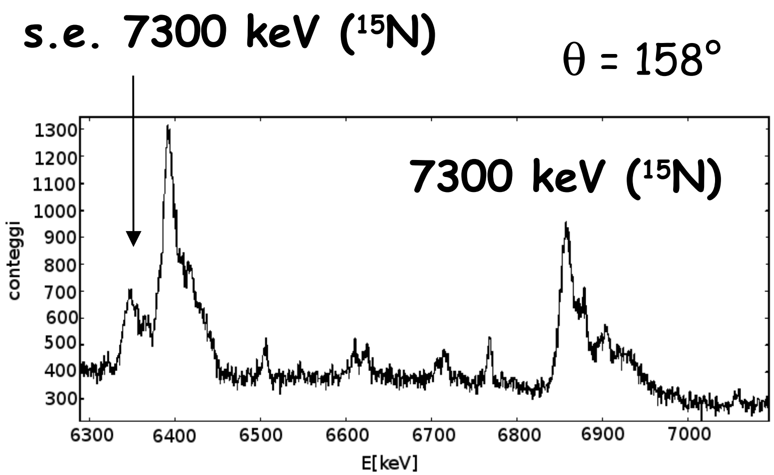

After subtraction of AmBe spectrum and 7300 keV s.e.

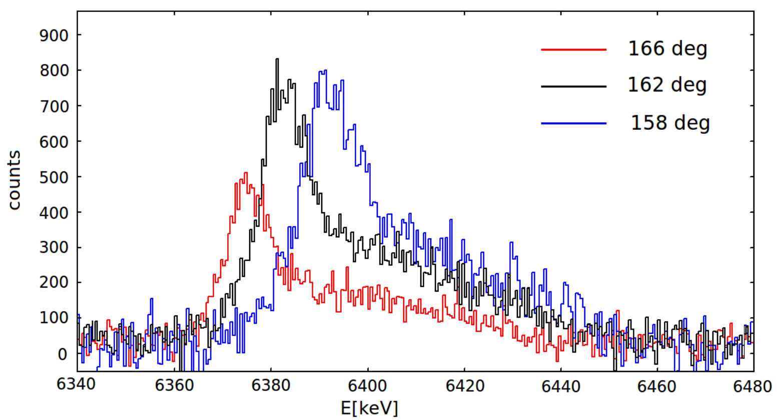

Line shape analysis is performed comparing experimental spectra with detailed simulations of the reaction mechanism and the gamma emission and detection

Differential cross sections are needed to reproduce the line shape

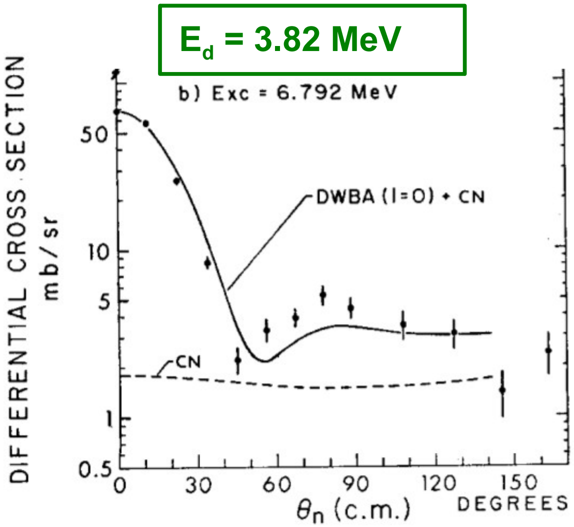

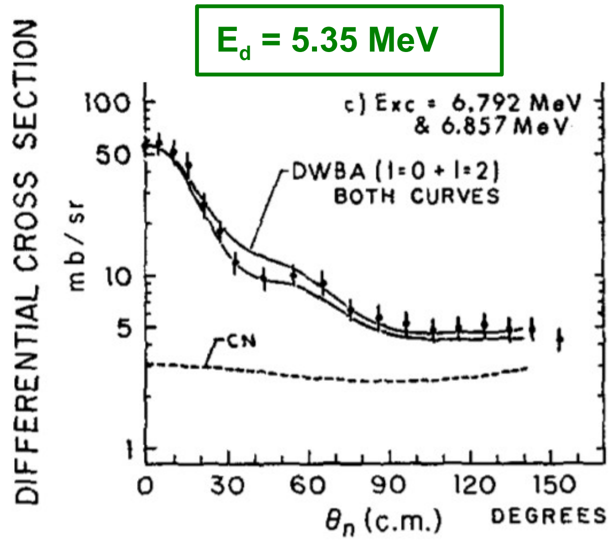

Ritter et al.
NPA 140 (1970) 609-624

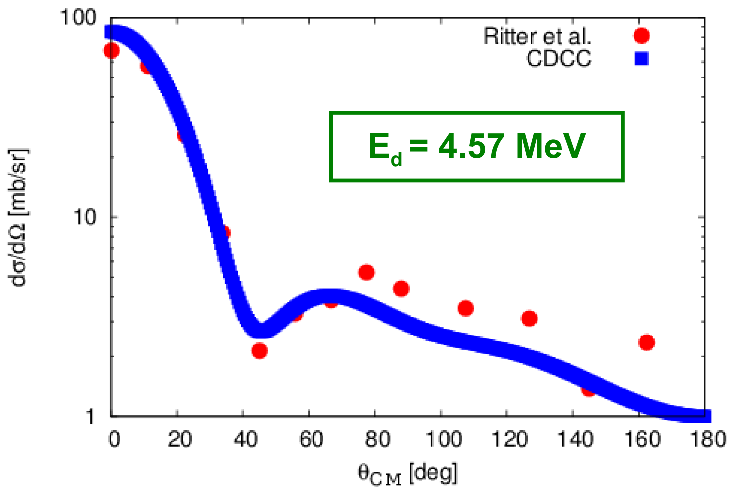

CDCC calculations (N. Keeley) provide the angular distribution at the exact experimental energy

Experiment VS Simulations

8312 keV (^{15}N), nucleon transfer (CDCC), τ = 1.73 fs

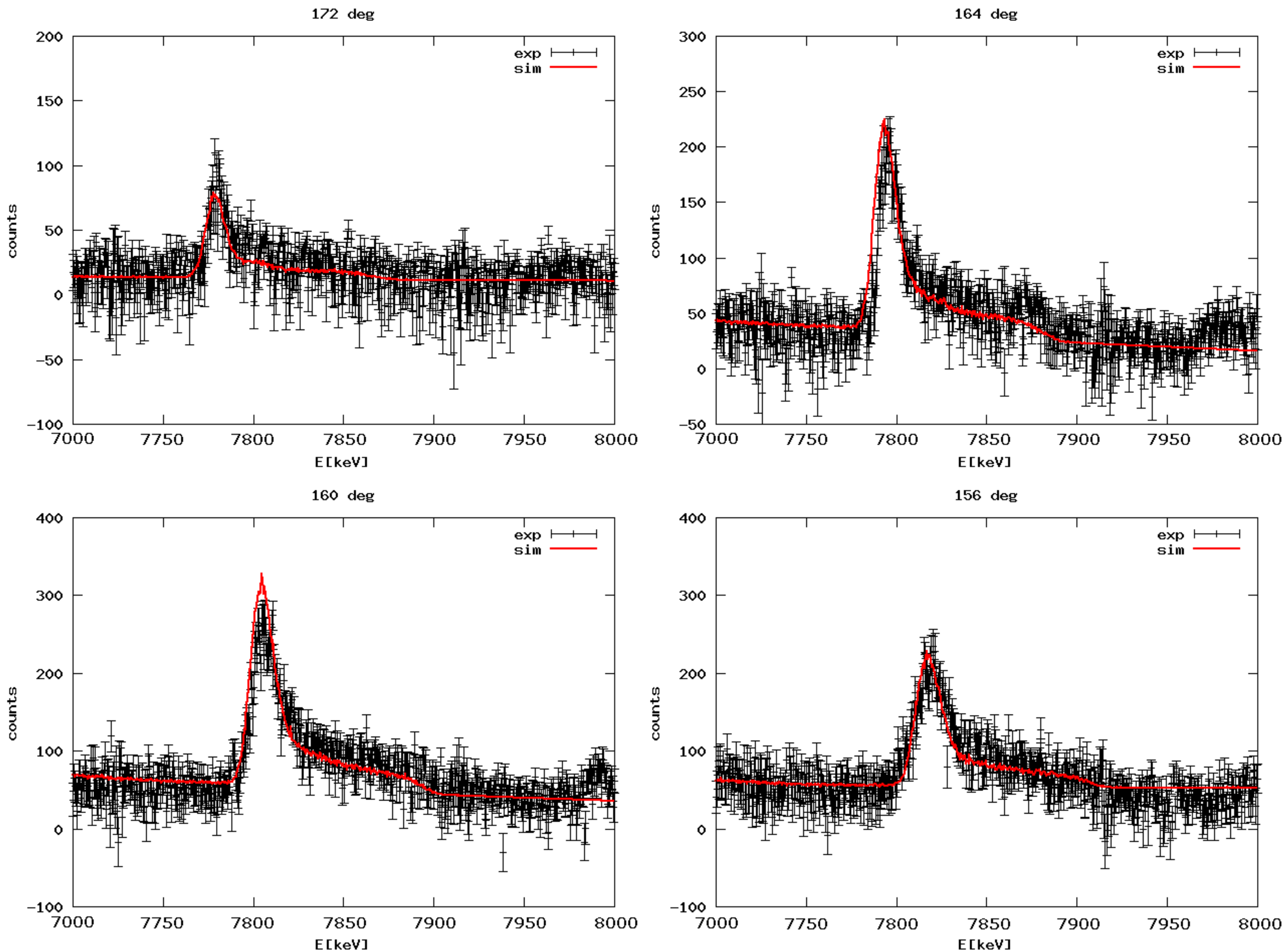

8312 keV (^{15}N), nucleon transfer (CDCC), τ = 1.73 fs

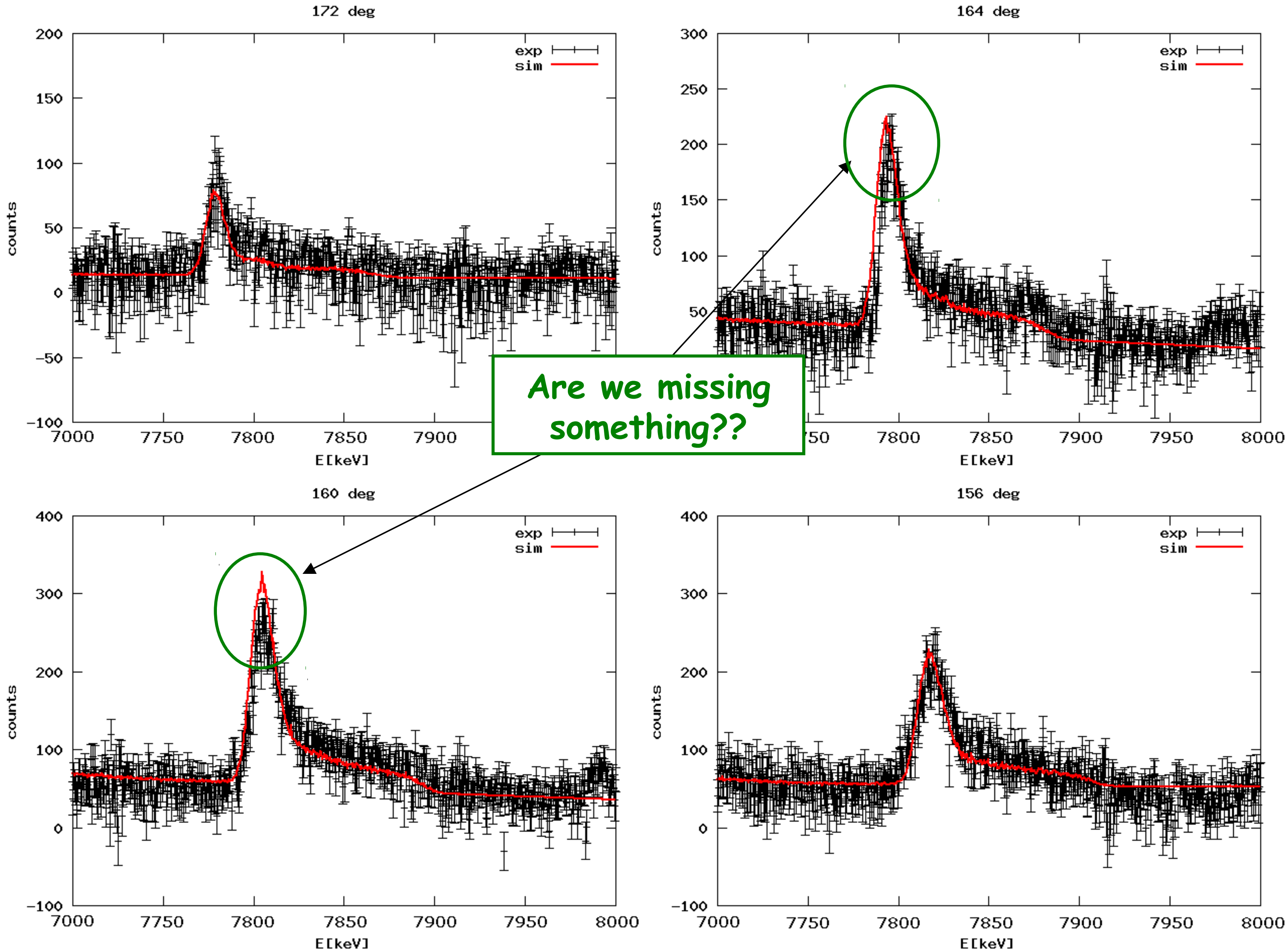

8312 keV (^{15}N), nucleon transfer + 20% fusion – evaporation

(E_p = 2MeV, σ_p = 1.5MeV)

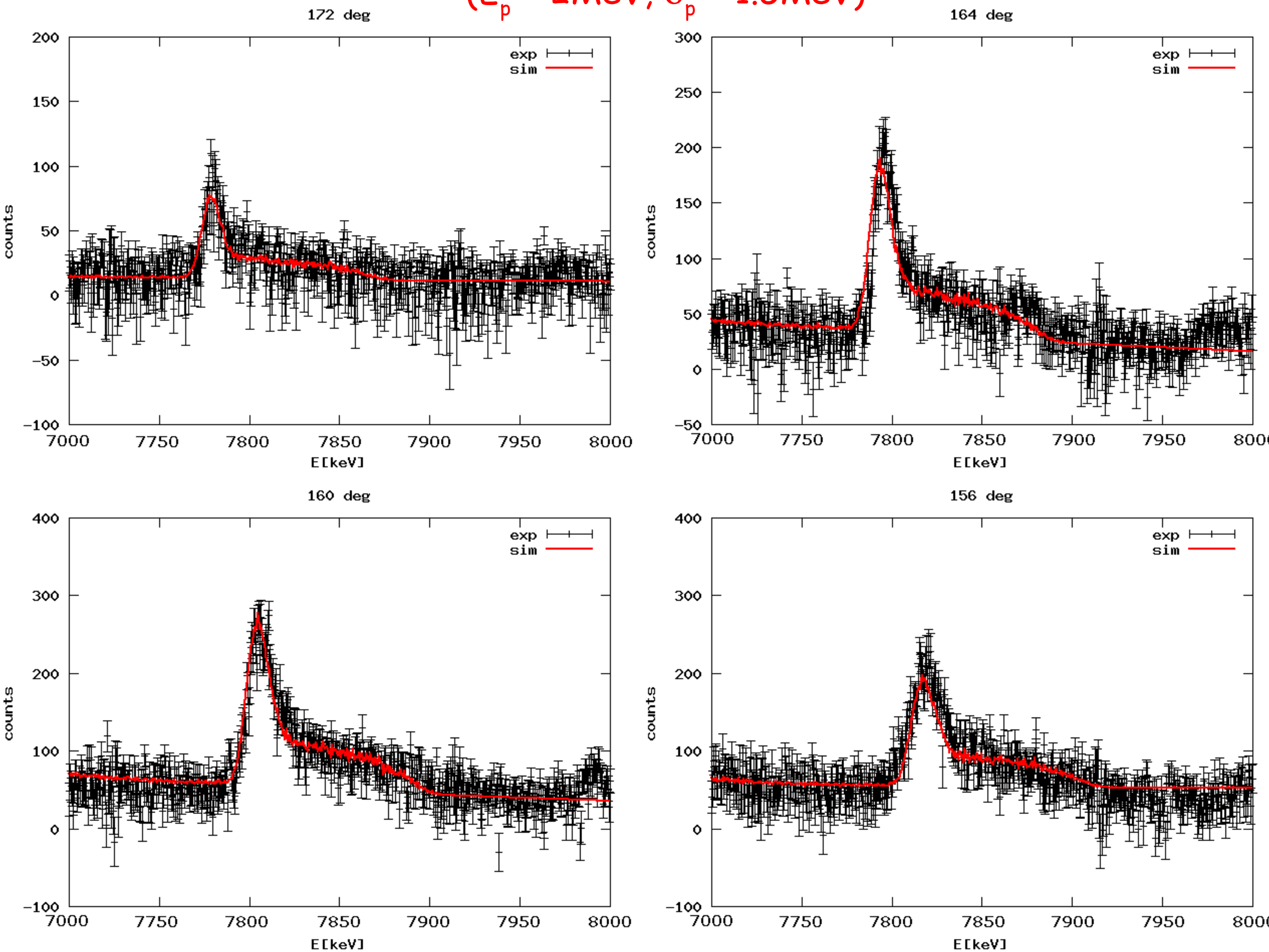

Experiment VS Simulations

6791 keV (^{15}O), nucleon transfer (CDCC), τ = 1 fs

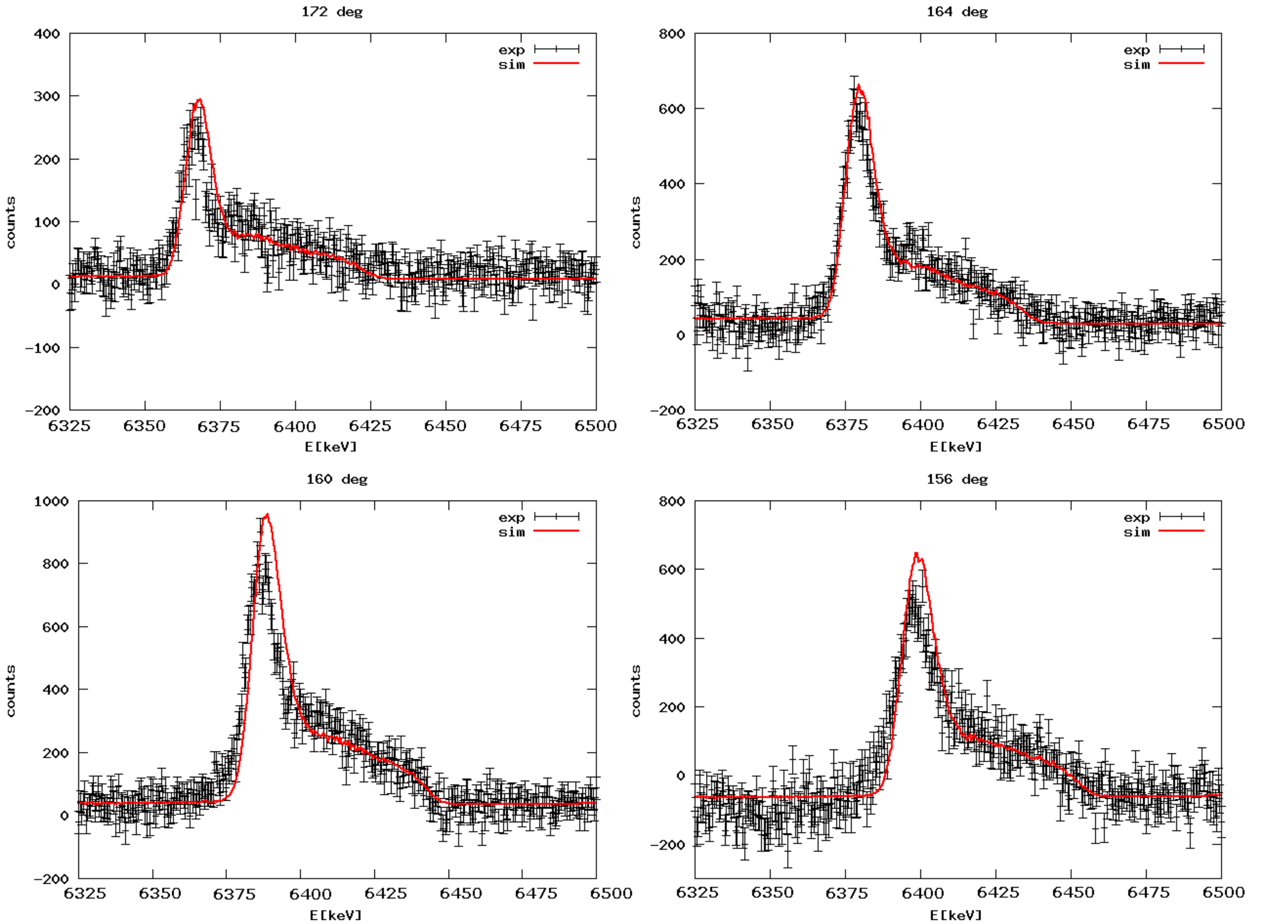

Experiment VS Simulations

6791 keV (^{15}O), nucleon transfer (CDCC), τ = 5 fs

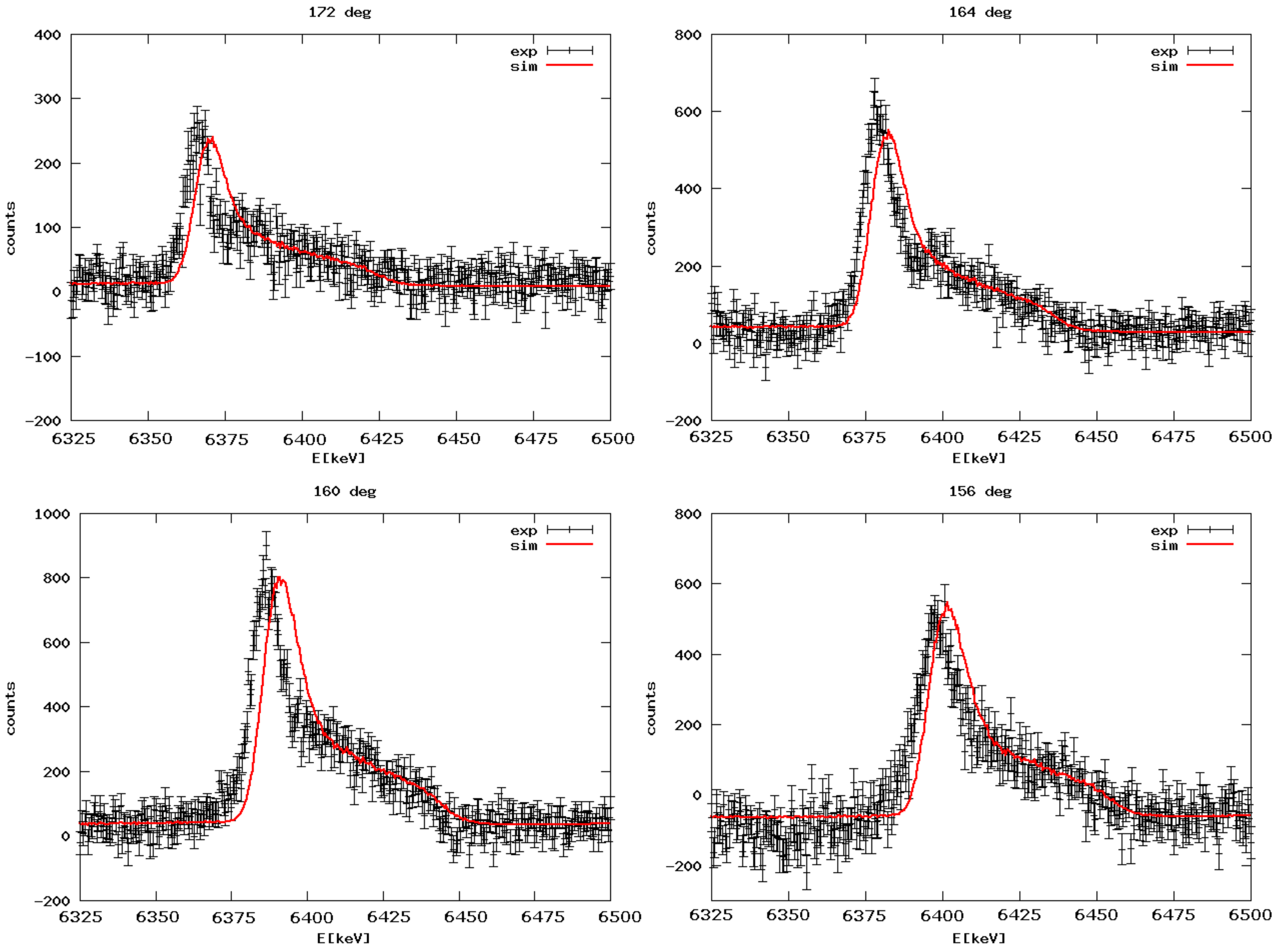

6791 keV (^{15}O), nucleon transfer + 20% fusion - evaporation, τ = 1 fs

(E_n = 2MeV, σ_n = 1.5MeV)

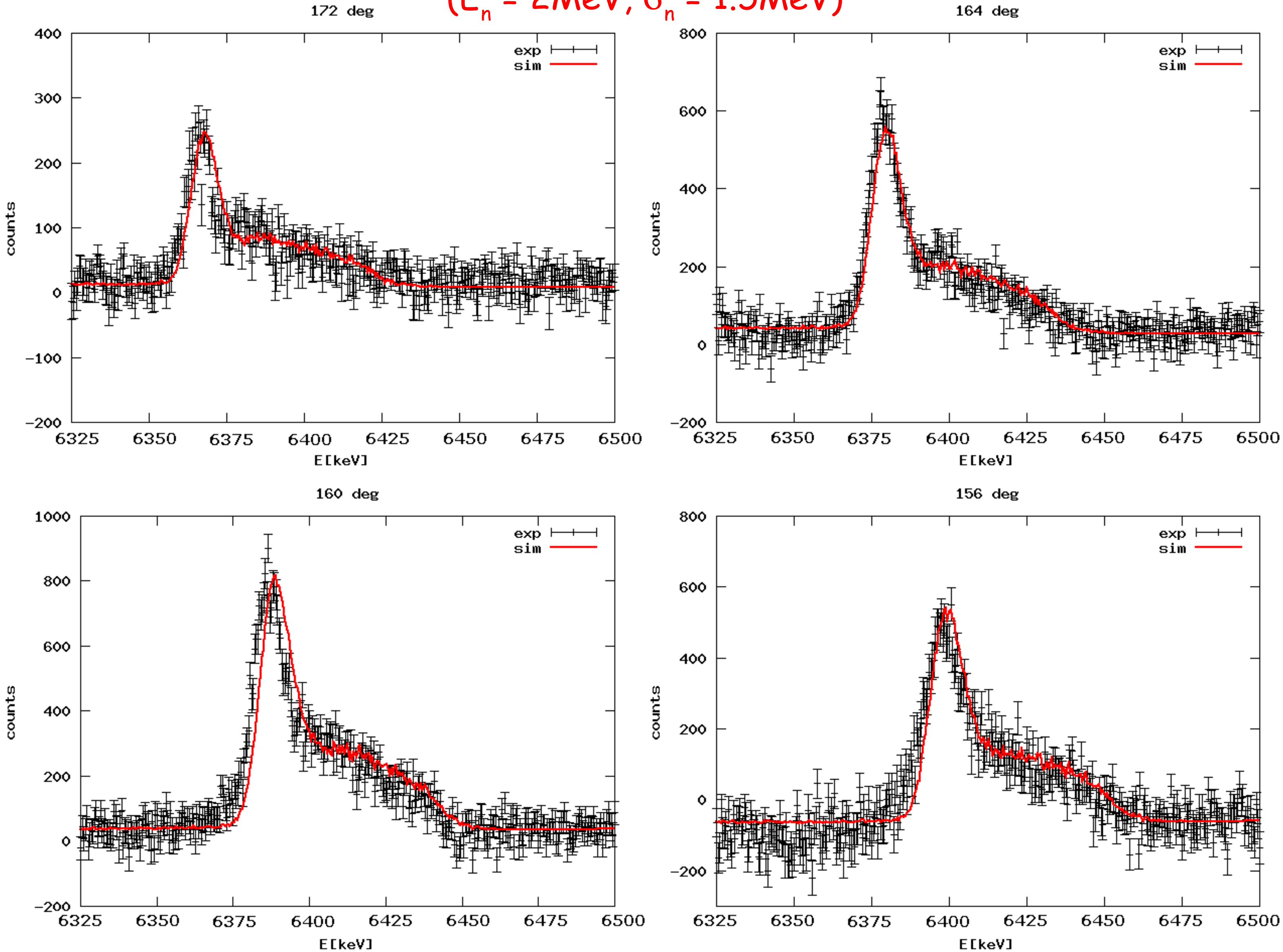

Conclusions

→ The high energy and angular resolution of the AD make the line shape sensitive to fs lifetimes

→ Lower upperlimit in the lifetime of the level of interest (~fs) with respect to what was obtained in the past with the same technique (Gill et al., NPA 121 (1968) 209).

→ The complex kinematics of the $^{2}H(^{14}N,n)^{15}O$ reaction limits the line shape sensitivity at sub-fs lifetimes

Future work:

→ Theoretical estimation of the fusion – evaporation cross section

→ χ^2 test to quantify the line shape sensitivity to the lifetime

→ Run again data processing in order to recover the signal of damaged segments (spectra will not change significantly)

SUPPLEMENTARY SLIDES

3D Solar atmosphere model

New 3D solar atmosphere models:
- → essentially parameters free
- → better fit of absorbtion lines
- → agreement with local intersetellar medium composition

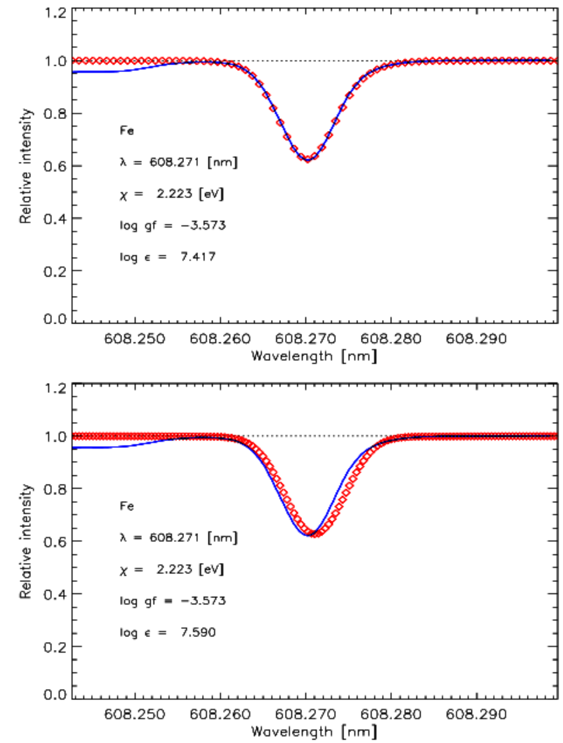

M. Asplund. astro-ph/0302407v1, 2003

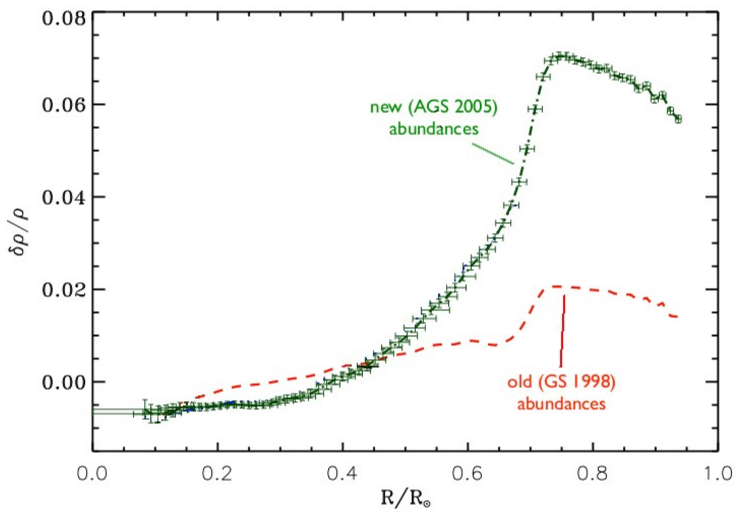

J.N. Bahcall et al.
The Astrophysical Journal, 618:1049 –1056, 2005

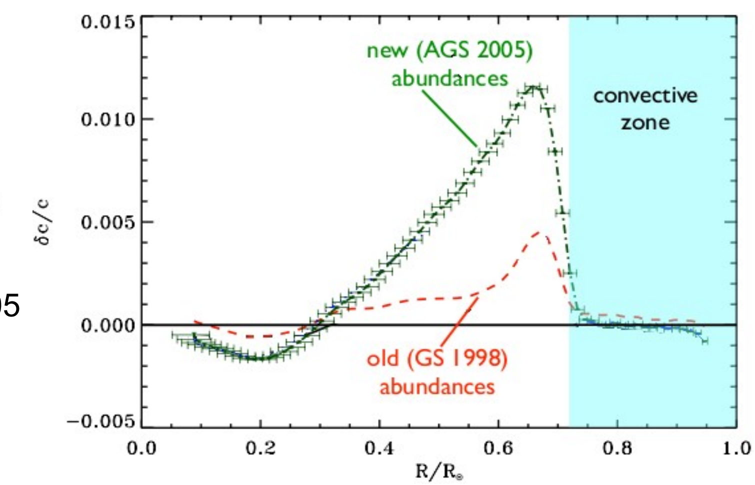

Age of globular clusters

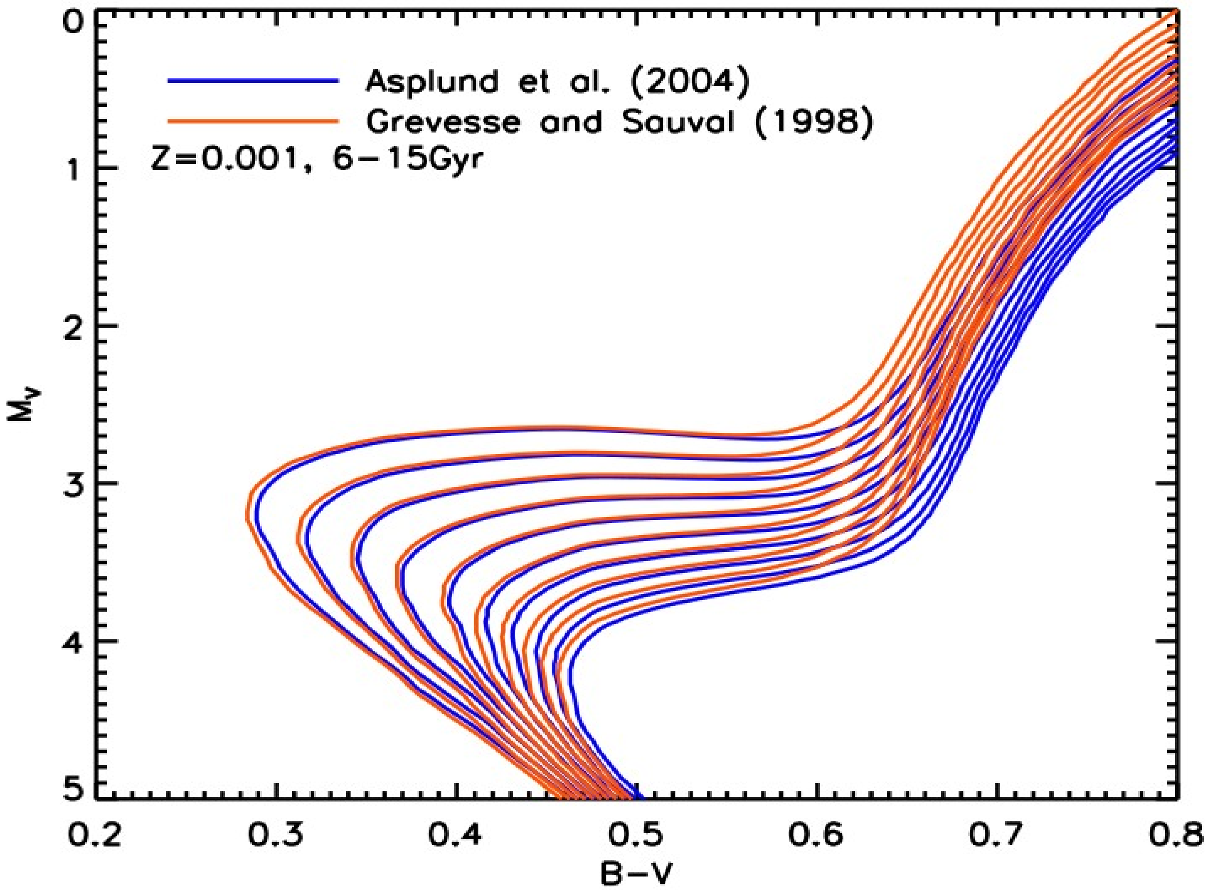

Sukyoung K. Yi and Yong -Cheol Kim
Journal of The Korean Astronomical Society 43: 135 ~ 139, 2010

Neutrino flux

C, N β_j			
Source	C	N	O
$\phi(^8B)$	0.027	0.001	0.107
$\phi(^{13}N)$	0.874	0.142	0.044
$\phi(^{13}N)/\phi(^8B)^{0.599}$	0.858	0.141	-0.020
$\phi(^{15}O)$	0.827	0.200	0.071
$\phi(^{15}O)/\phi(^8B)^{0.828}$	0.805	0.199	-0.018

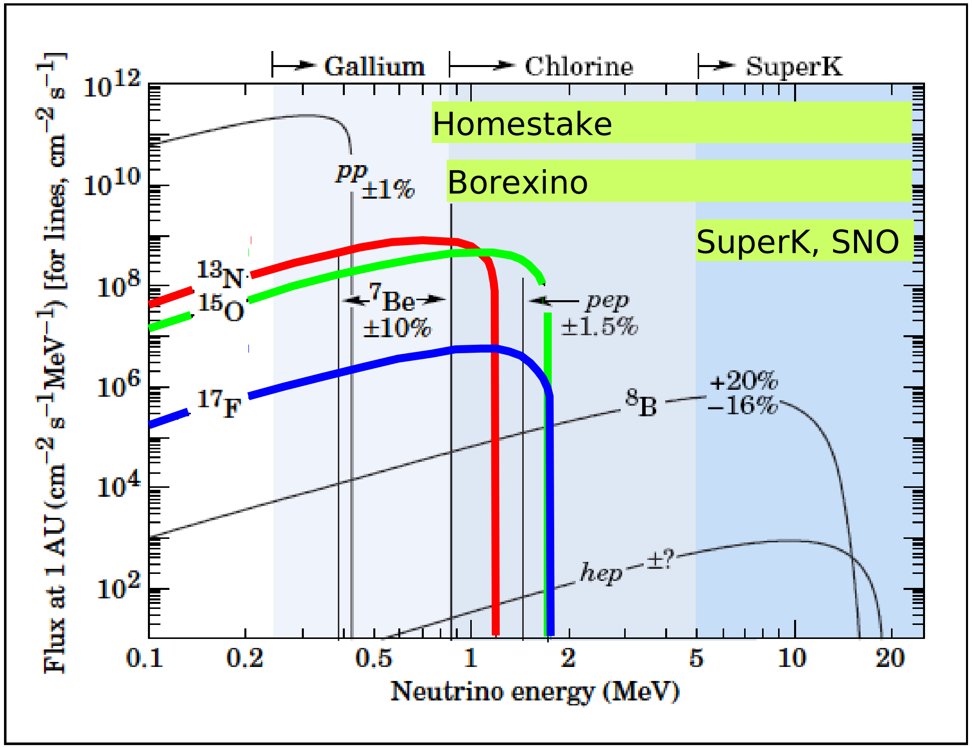

	Environmental β_j				Nuclear β_j					
Source	$L_\odot$	Opacity	Age	Diffusion	S_{11}	S_{33}	S_{34}	S_{17}	S_{e7}	S_{114}
$\phi(^8B)$	7.16	2.70	1.38	0.28	-2.73	-0.43	0.85	1.0	-1.0	-0.020
$\phi(^{13}N)$	4.40	1.43	0.86	0.34	-2.09	0.025	-0.053	0.0	0.0	0.71
$\phi(^{13}N)/\phi(^8B)^{0.599}$	0.11	-0.19	0.03	0.17	-0.45	0.28	-0.56	-0.60	0.60	0.72
$\phi(^{15}O)$	6.00	2.06	1.34	0.39	-2.95	0.018	-0.041	0.0	0.0	1.00
$\phi(^{15}O)/\phi(^8B)^{0.828}$	0.07	-0.18	0.20	0.16	-0.69	0.37	-0.74	-0.83	0.83	1.02

$S_{14,1}$ cross section

$$\Phi_\nu^{CN} = f(\, S_{14N+p},\ T,\ CN\,)$$

Measurable (SNO+, Borexino)

Calibrated to 0.5% Using ^8B ν flux

Photospheric absorbition lines, Meteorites Helioseismology

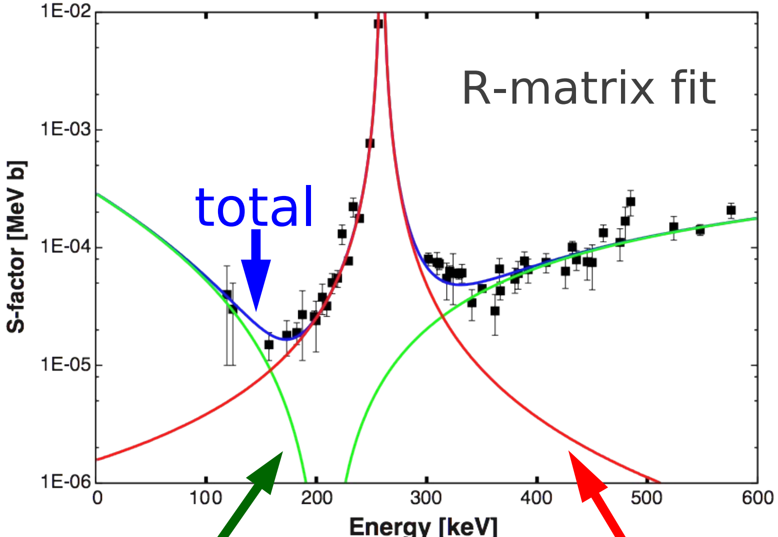

subthreshold resonance + external contribution

259 keV resonance alone

Γ_γ (6792 keV) = 0.6 eV, 0.8 eV, 1.0 eV

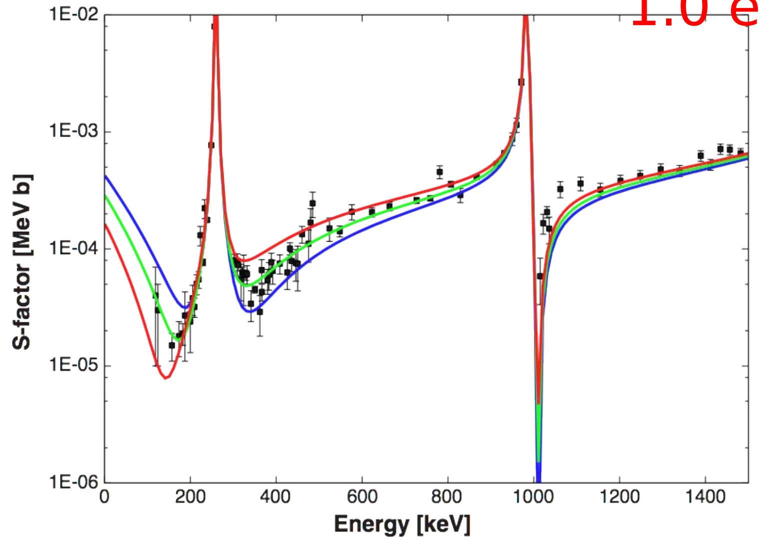

Pair production spectrum (sum of all angles)

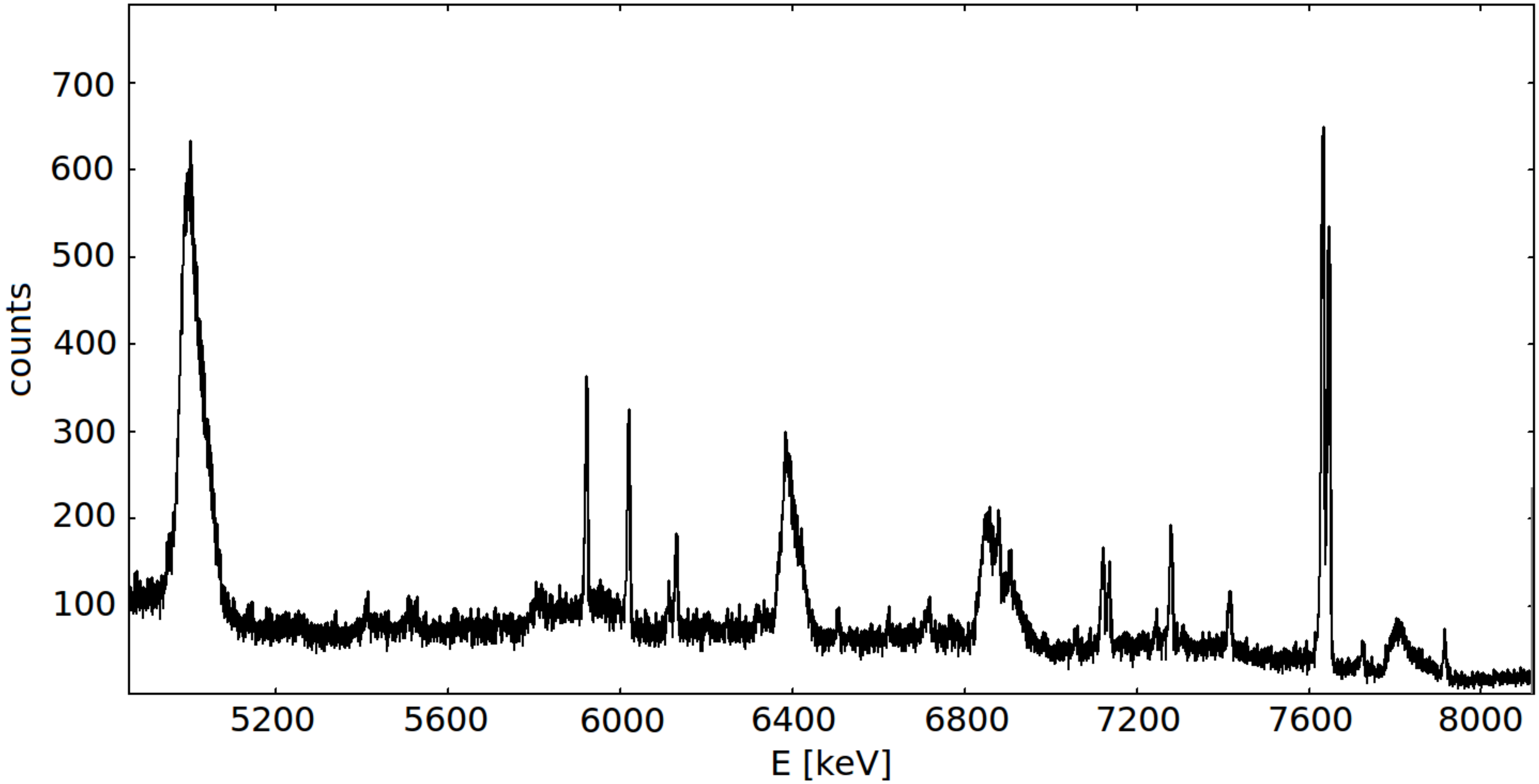

Energy resolution would maybe be better but statistics is poor

Gamma - gamma

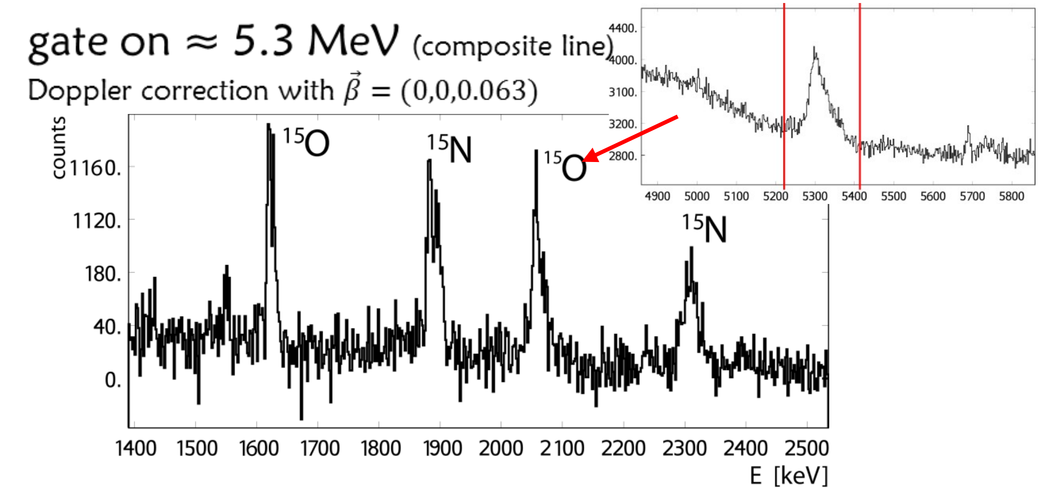

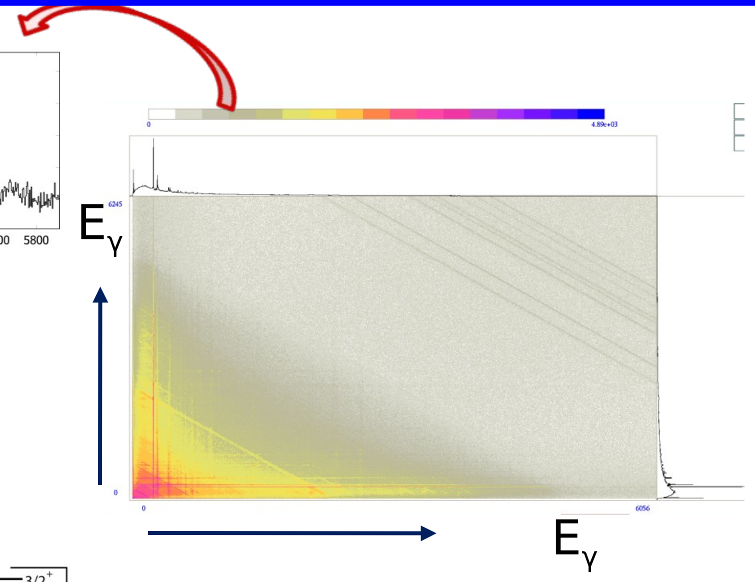

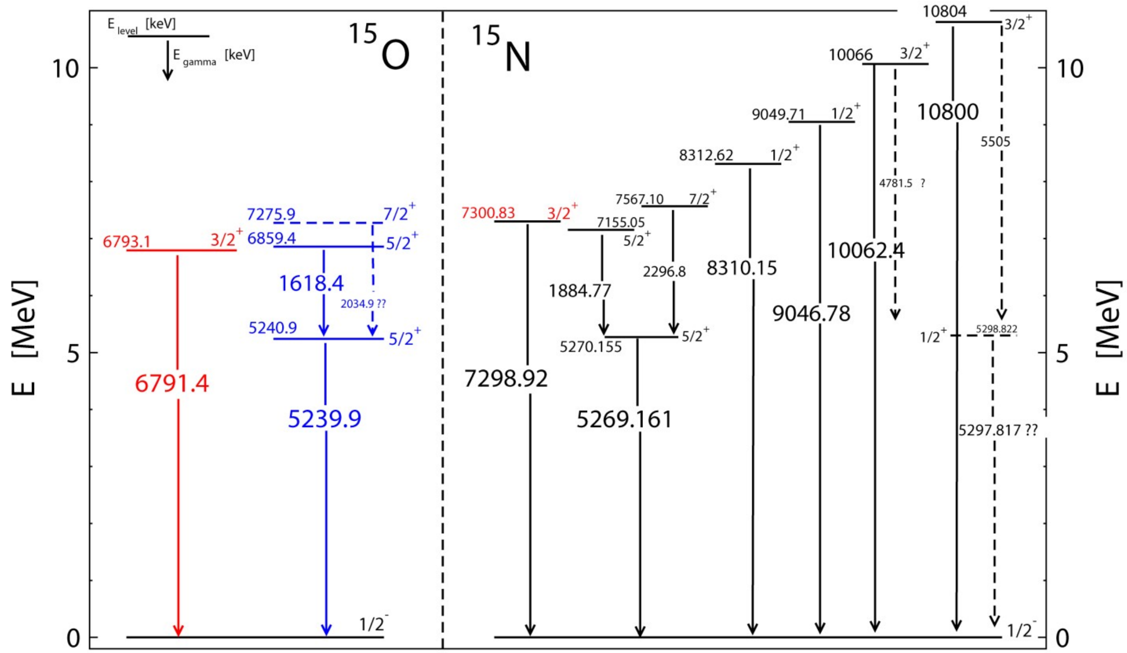

The main reaction channels are ^{15}O (Q = 5072 keV) and ^{15}N (8069 keV)

Experiment VS Simulations

6791 keV (^{15}O) CDCC τ = 0.5fs

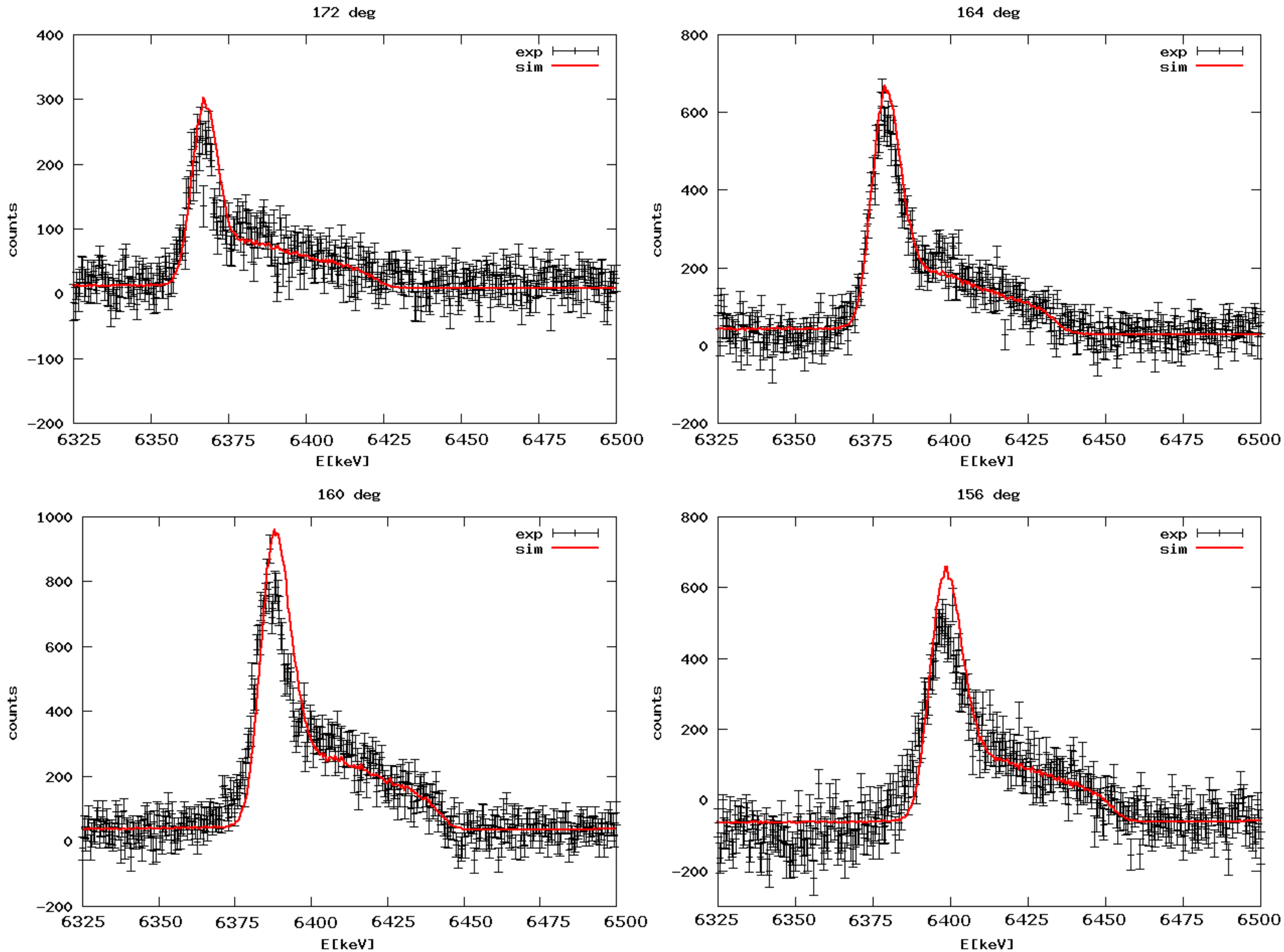

Experiment VS Simulations

6791 keV (^{15}O) CDCC τ = 2fs

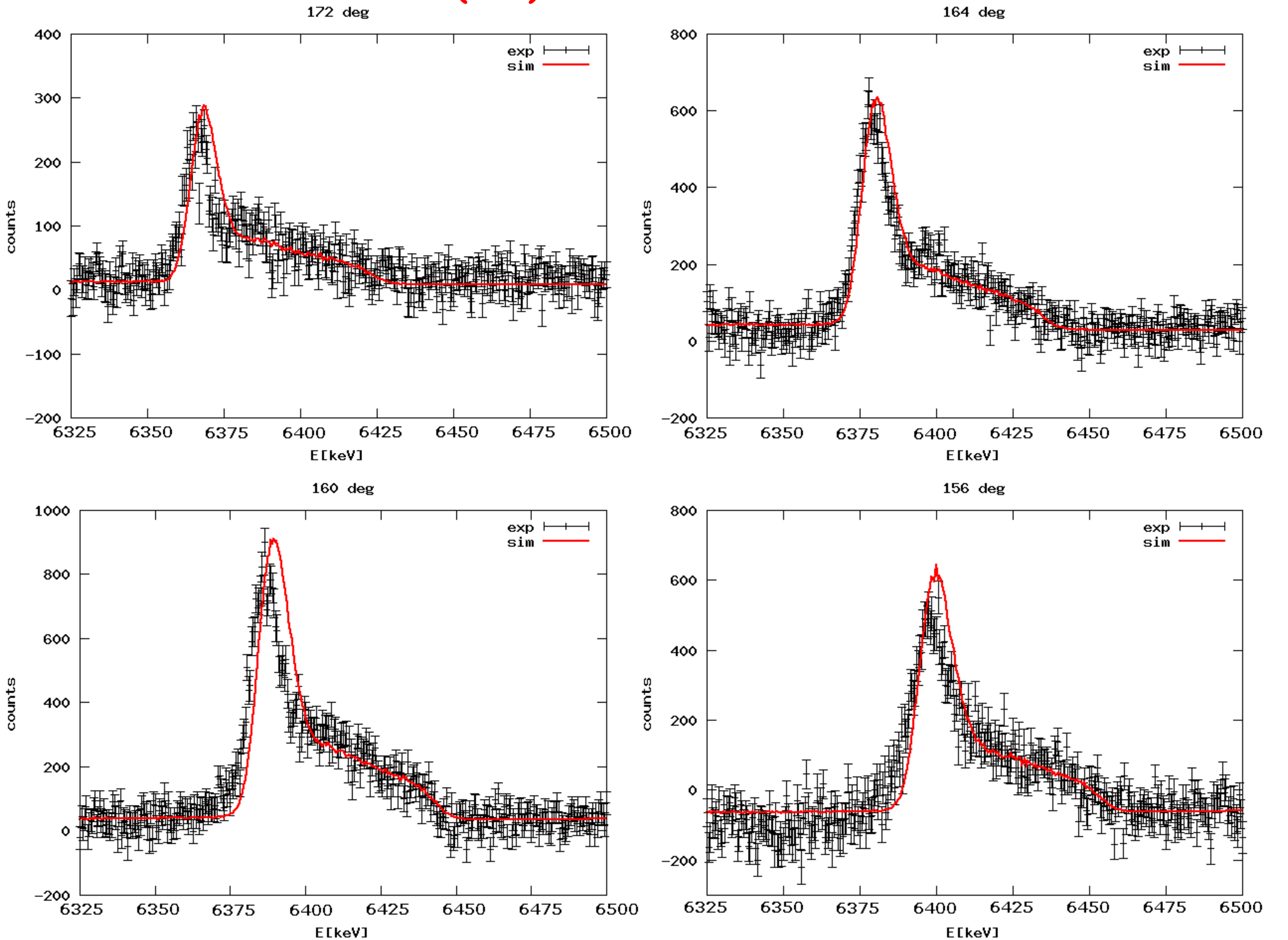

Experiment VS Simulations

6791 keV (^{15}O), nucleon transfer + 20% fusion – evaporation, τ = 5 fs

(E_n = 2MeV, σ_n = 1.5MeV)

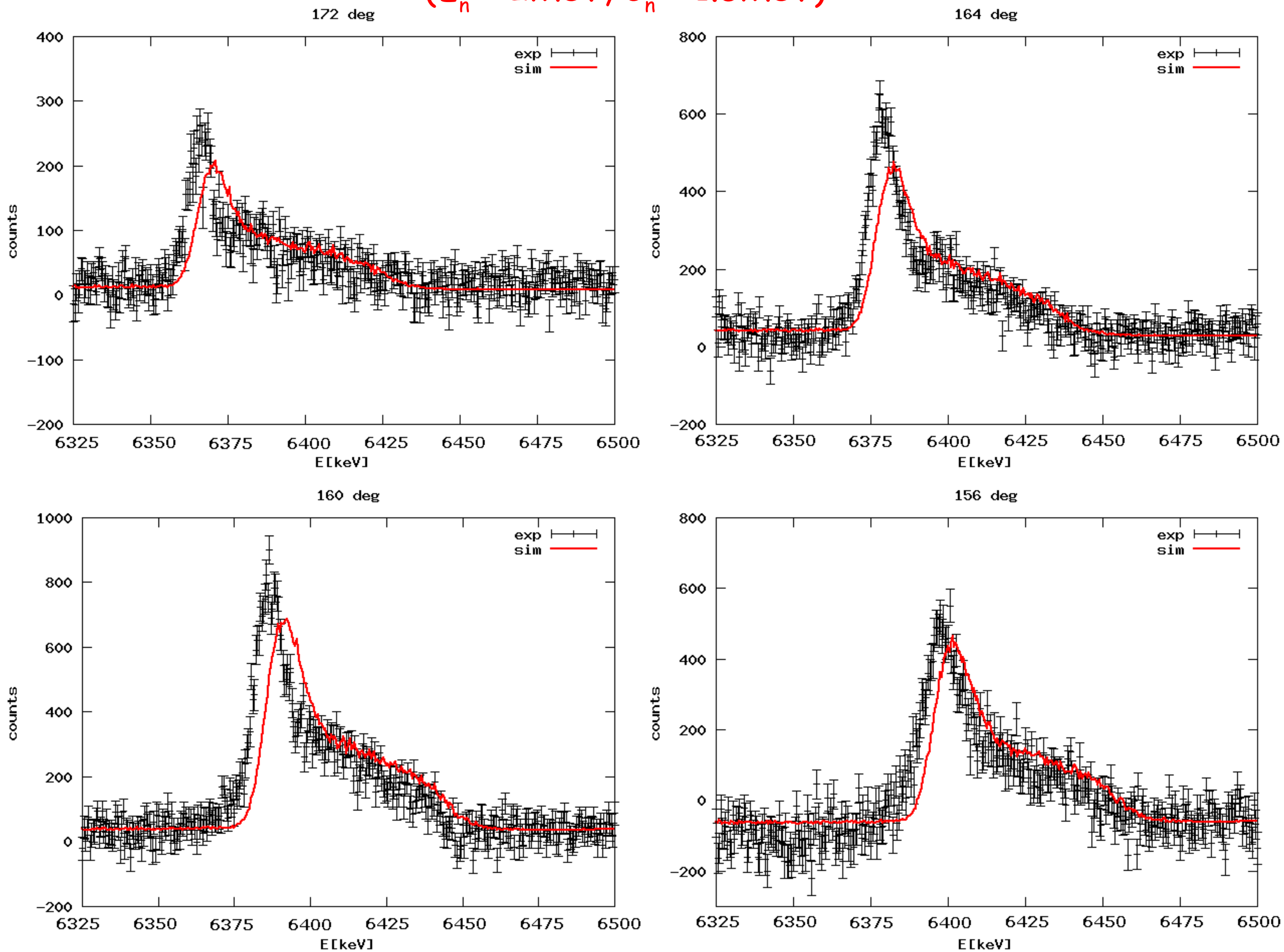

8310 keV differential cross section

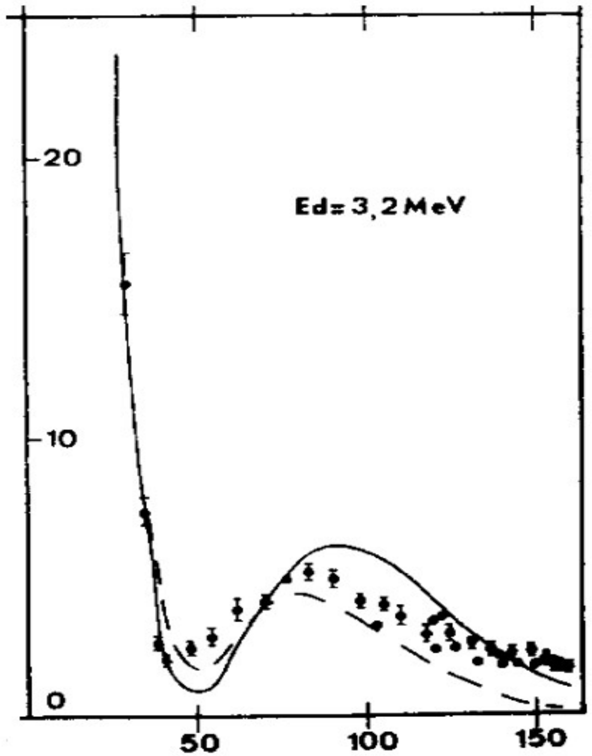

Beaumevieille et al.
NPA125 (1969) 568-584

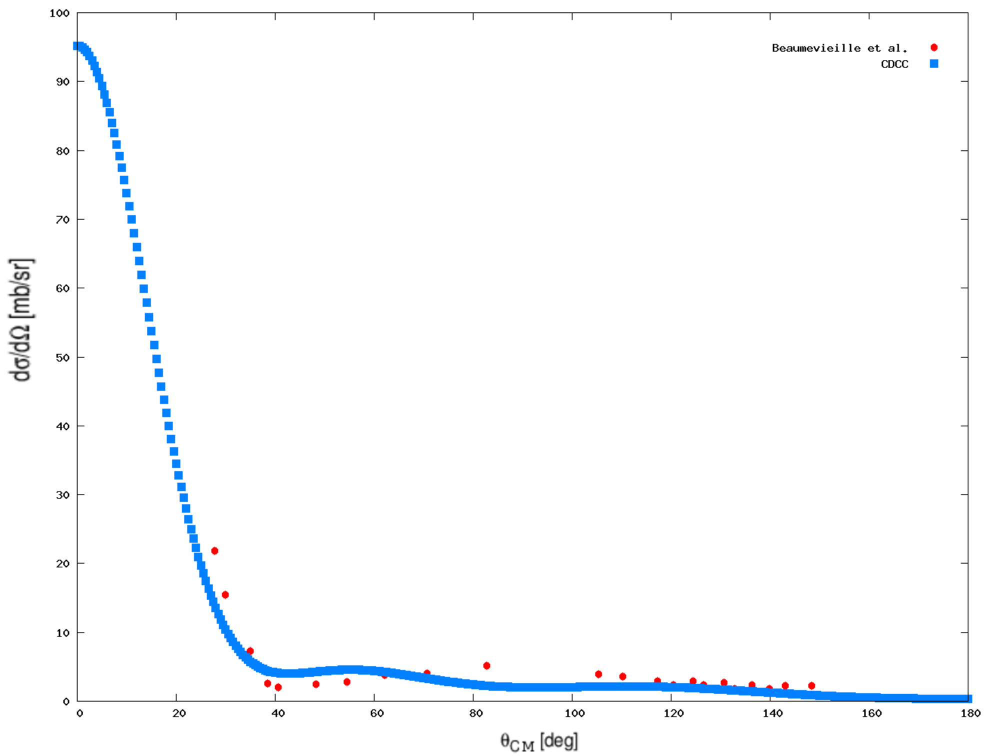

ERDA and RBS target analysis

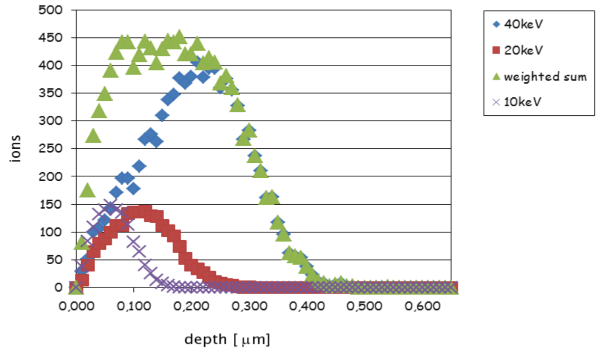

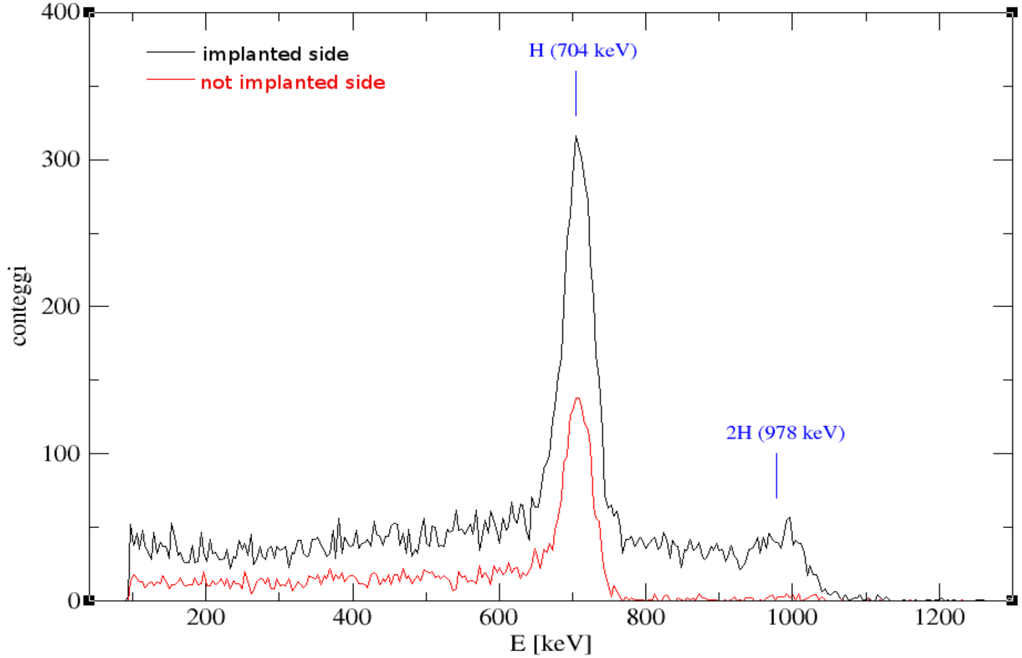

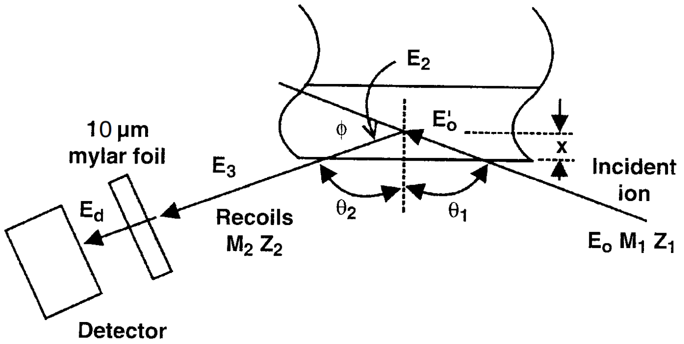

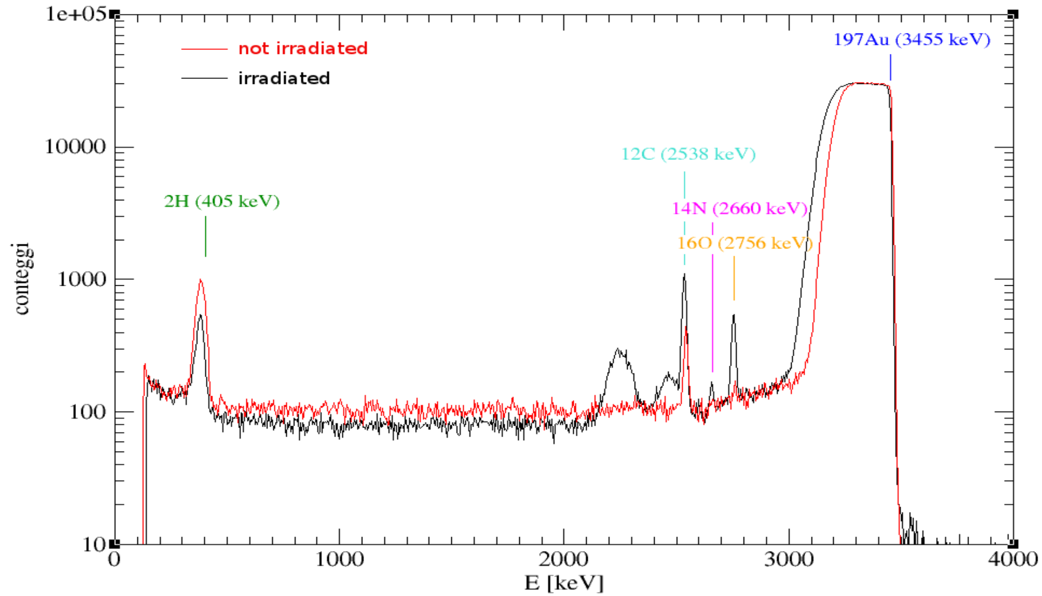

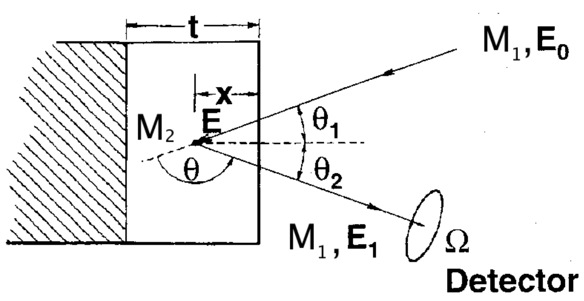

Data analysis: data processing

- Energy calibration of CC and segments with high energy gammas
  - Off-line refinement was needed to align the CC spectra
  - Non linearity of segments signals in the low gain range

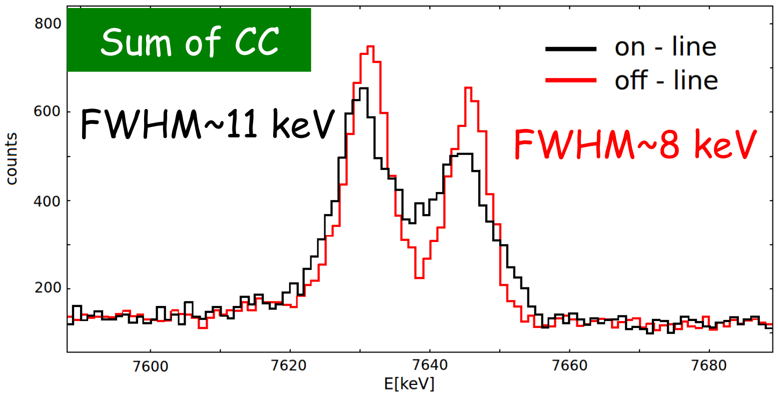

- PSA provides (E, x, y, z, t) of the interaction points for each crystal

- Tracking (at global level) provides the position of the first interaction point.
  - Performed forcing the sum of the energy releases of the tracked points to be equal to the corresponding energy seen in the CC

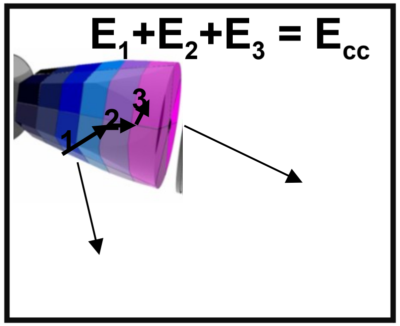

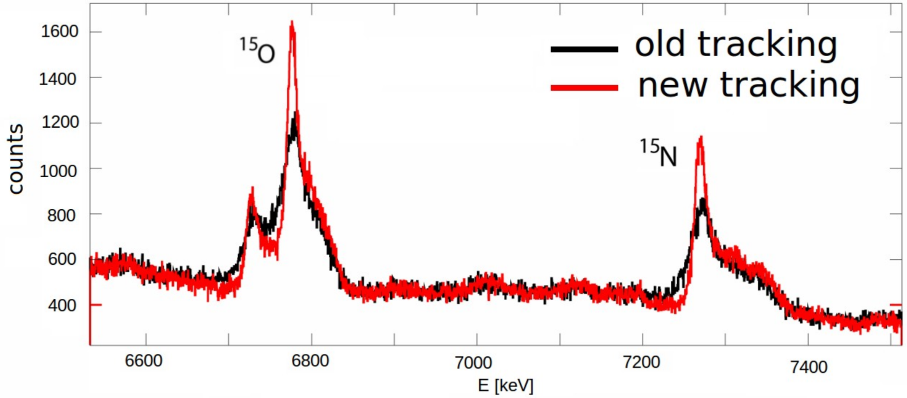

- Crystals 1R and 2R excluded from the analysis for 65% of the experiment because of desynchronization